CHEMISTRY
A European Journal

A Journal of
ChemPubSoc Europe

Accepted Article

Title: REDOX-SWITCHABLE CALIX[6]ARENE-BASED ISOMERIC ROTAXANES

Authors: Valeria Zanichelli, Margherita Bazzoni, Arturo Arduini, Paola Franchi, Marco Lucarini, Giulio Ragazzon, Andrea Secchi, and Serena Silvi

To be cited as: *Chem. Eur. J.* 10.1002/chem.201800496

Link to VoR: http://dx.doi.org/10.1002/chem.201800496

Supported by
ACES

WILEY-VCH

10.1002/chem.201800496

WILEY-VCH

REDOX-SWITCHABLE CALIX[6]ARENE-BASED ISOMERIC ROTAXANES

Valeria Zanichelli,[a] Margherita Bazzoni,[a] Arturo Arduini,[a] Paola Franchi,[b] Marco Lucarini,[b] Giulio Ragazzon,[b,c],* Andrea Secchi[a],* and Serena Silvi[b],*

Abstract: Operating molecular machines are based on switchable systems, whose components can be set in motion in a controllable fashion. The presence of non-symmetric elements is a mandatory requirement to obtain and demonstrate the unidirectionality of motion. Calixarene-based macrocycles have proven very efficient hosts in the design of oriented rotaxanes and of pseudorotaxanes with a strict control on the direction of complexation. We have synthesized and characterized a series of two-station rotaxanes based on bypiridinium-ammonium axles. We have exploited a recently reported supramolecular-assisted strategy for the synthesis of different orientational isomers and we identified the ammonium unit as a proper secondary station for the calixarene. We were able to trigger the displacement of the macrocycle upon electrochemical reduction of the bipyridinium primary station and we demonstrated that the shuttling is influenced both by the length of the chain of the axle component and by the position of the secondary station with respect to the calixarene rims.

Introduction

In the field of molecular level machines, the possibility to synthesize and operate with supramolecular systems capable of performing specific movements under the action of a defined external energy input constitutes a fascinating challenge.[1–5] One of the simplest classes of molecular machines is represented by molecular shuttles based on rotaxane architectures, which were first characterized by Stoddart et al. in solution in 1991.[6] Since that report, many mechanically interlocked molecules have been designed, synthesized and shown to mimic the complex functions of macroscopic switches with a wide range of applications, including molecular electronic devices, sensors, nanomechanical systems and instruments capable of delivering both chemical and biological cargos in a controlled manner.[7–10] The shuttling motion can be triggered by a plethora of different stimuli,[4,11] such as thermal treatment,[12] ion coordination,[13,14] electrochemical[15] or photochemical[16,17] activation, changes of solvent or pH.[18] In order to obtain work from a molecular machine, and to move from switches to real molecular motors, full control on the direction of motion must be attained.[19–22] This is one of the main challenges when designing a molecular machine and it involves the exploitation of inherently non-symmetrical components, arranged in univocally oriented architectures. Indeed, asymmetry is a fundamental factor in the majority of systems reported to date, not only for obtaining unidirectionality of motion, but also for demonstrating it.[23]

In a rotaxane-based architecture, asymmetry can be included both in the axle and wheel components. The majority of two-station molecular shuttles reported so far is based on non-symmetric axles,[18,24,25] but in principle the direction of motion in a rotaxane could be dictated by the asymmetry of the wheel component (Figure 1).[22,26–31] In a minimalistic design like the one reported in Figure 1a, upon weakening the interaction between the axle and the ring the formation of two orientational isomers could be envisaged. If the non-symmetric ring has a preferential direction of motion, dictated by the different nature of its two rims, then it would be possible to get selectively only one orientational isomer. If both the axle and the ring are non-symmetric (Figure 1b), then two orientational isomers can be synthesized, and the movement of the ring can give rise to four translational isomers (Figure 1b).

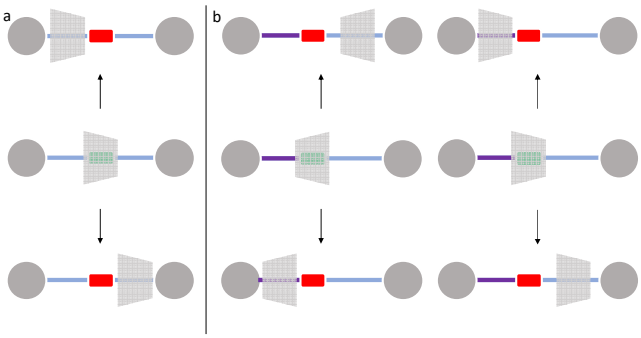

Figure 1. Rotaxanes with a) a symmetric axle and non-symmetric ring and b) both non-symmetric components (two orientational isomers): on weakening the interaction between the axle and the ring, different translational isomers can be obtained, depending on the direction of motion of the ring.

[a] Dr. V. Zanichelli, Margherita Bazzoni, Prof. A. Arduini, Prof. A. Secchi
Dipartimento di Scienze Chimiche, della Vita e della Sostenibilità Ambientale
Università di Parma
Parco Area delle Scienze 17/A, I-43124 Parma, Italy
E-mail: andrea.secchi@unipr.it
[b] Dr. P. Franchi, Prof. M. Lucarini, Dr. G. Ragazzon, Dr. S. Silvi
Dipartimento di Chimica "G. Ciamician",
Università di Bologna
Via Selmi 2, I-40126, Italy
E-mail: serena.silvi@unibo.it
[c] Dr. Giulio Ragazzon
Dipartimento di Scienze Chimiche
Università di Padova
via Marzolo 1, I-35131, Padova
E-mail: giulio.ragazzon@unipd.it

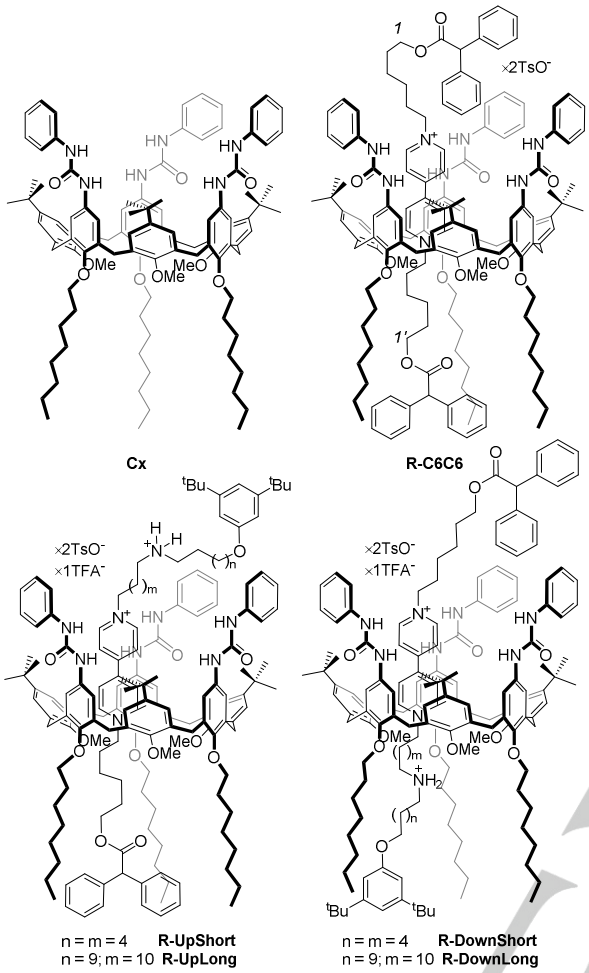

Figure 2. Single and double-station rotaxanes derived from calix[6]arene **Cx**.

We have exploited the complexation abilities of calix[6]arene derivative **Cx** (Figure 2) toward 4,4'-bipyridinium-based axles[32,33] to synthesize non-symmetric rotaxanes. In these systems, both the axle and the wheel components are non-symmetric (Figure 1b):[33] the calixarene presents two rims which are functionalized with three *N*-phenylureido groups (upper rim) and three octyl chains (lower rim), and differ for both size and chemical properties, and the dumbbells are decorated with two alkyl chains with an appropriate difference in length. Moreover, in each molecule, the components are arranged in a univocal and controlled relative orientation, giving rise to constitutionally isomeric oriented rotaxanes. Since the functionalized calixarene is non-palindrome, the movement of the wheel towards one side of the axle would be chemically not equivalent to the one towards the opposite side and could therefore generate specific translational isomers (Figure 1b). We first planned to induce the shuttling by exploiting the response of these redox-active systems to electrochemical stimulation.[33] However, it emerged that the sole electrochemical reduction of the bipyridinium core is not sufficient to induce any mechanical rearrangement in these rotaxanes. Cyclic voltammetry and EPR measurements showed that, contrarily to what observed for similar pseudorotaxane assemblies,[34] no detectable movement of the macrocyclic component takes place when the axle is mechanically interlocked in a rotaxane-type structure,[32] regardless of the nature and the orientation of the threaded dumbbell.[33] From these results, it emerged that the presence of a further recognition element is mandatory to facilitate the displacement and promote the shuttling. We thus focused our attention on double-station rotaxanes, equipped with two distinct recognition sites (*stations*) on their dumbbell-shaped component, in which the macrocycle can move from one site to the other in a controlled and reversible manner. To achieve this goal, it is crucial that the two stations exhibit a different association strength with the receptor. If this is the case, the rotaxane can exist as two different equilibrating co-conformations, the populations of which reflect their relative free energies, determined by the extent of the two different sets of non-covalent bonding interactions. To this aim, in this paper we tackled the synthesis of a series of novel double station rotaxanes, constituted by the calix[6]arene wheel **Cx** and dialkylviologen-based axles endowed with an ammonium station as second recognition unit on the dumbbell (see Figure 2).

Results and Discussion

Synthesis of rotaxanes

To describe the results of this study, we labeled the compounds with descriptors showing (i) the position of the ammonium station with respect to the rims of the calixarene (**Up** if the station is oriented towards the upper rim, **Down** if it is oriented towards the lower rim), (ii) the length of the *N*-containing side chain connected to the pyridinium nitrogen atom (**Long** or **Short**) (see Figure 2). Labels **DB**, **P** and **R** denote, respectively, dumbbells, pseudorotaxanes and rotaxanes. To gain information about a possible preferential shuttling direction, pivoted by the inherent asymmetry of **Cx**, we designed two different series of orientational rotaxane isomers in which the ammonium station (*N*-station) faces the two opposite rims of the macrocycle. To have an insight about the influence of the length of the spacers, and to assure that the movement is not impeded by neighbouring molecular components, each series was synthesized with a long ($C_{12}NC_{11}$) and a short (C_6NC_6) side chain (Figure 2). Taking inspiration from the previously followed protocols,[33] we designed the synthesis of axles endowed with a bulky stopper at one end, and a terminal OH group appended at the opposite side. For the preparation of the rotaxanes having the longer *N*-containing side chain toward the calixarene upper rim, the appropriate *N*-Boc protected axles **6a** and **6b** were synthesized according to Scheme 1. *N*-Boc protected ω-aminoalcohols **1a-b** were converted in tosylates **2a-b**. These latter were first reacted with 3,5-di-*tert*-butylphenol in the presence of K_2CO_3 to insert the stopper (**3a-b**) and then with a molar excess of either 1,6-dibromohexane or 1,12-dibromododecane to complete the backbone of the *N*-containing alkyl side chains. Reaction of the resulting bromides **4a-b** with the pyridyl pyridinium tosylate **5** finally afforded axles **6a** and **6b** in 46% and 50% yield, respectively (see Experimental).

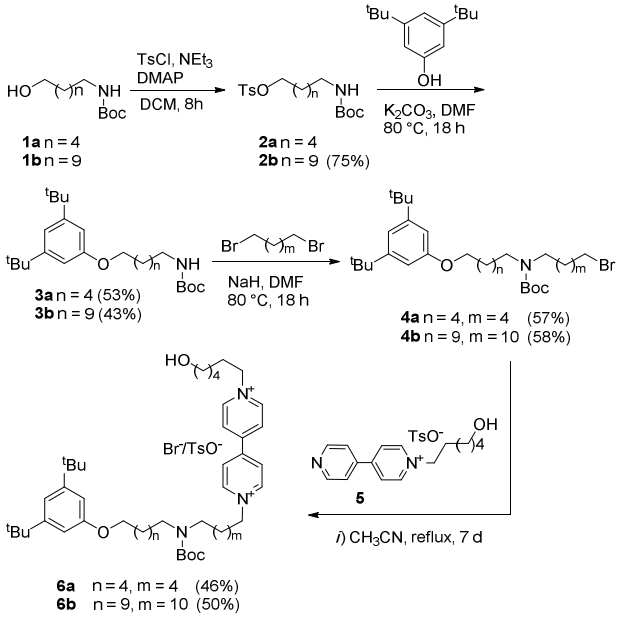

Scheme 1. Synthesis of *N*-Boc protected axles **6a** and **6b**.

In separated experiments, these axles were then equilibrated at room temperature in toluene with an equivalent of wheel **Cx**. After stirring for three hours at room temperature, the initial suspensions gradually turned homogeneous and red coloured. This coloration is usually ascribed to the charge transfer interaction occurring in a pseudorotaxane complex between the viologen core of the axle and the π-rich aromatic cavity of the calixarene. As shown in previous studies,[35,36] the presence on the axle of a terminal bulky stopper leads to the unidirectional threading of the axle from the upper rim of **Cx** with its ω-hydroxy hexyl chain and thus to the exclusive formation of oriented pseudorotaxanes **P-UpShort** and **P-UpLong** as depicted in Scheme 2. The subsequent axle stoppering reaction with diphenylacetylchloride, carried out directly in the toluene solution of each psuedorotaxane, followed by treatment with trifluoroacetic acid of the dichloromethane solutions of the resulting *N*-Boc protected rotaxanes, allowed us to eventually isolate the desired rotaxanes **R-UpShort** and **R-UpLong** in 55% and 27% of overall yield, respectively (see Scheme 2).

For the preparation of the orientational rotaxane isomers having the *N*-station facing the lower rim of the calixarene wheel (**R-DownLong** and **R-DownShort** in Figure 2), we designed the synthesis of axles **11a** and **11b**, which are endowed with the secondary ammonium function between the viologen unit and the terminal OH group (see Scheme 3). In the first step, the hydroxyl group of **1a-b** was protected with *tert*-butyldimethylsilyl chloride (TBSCl), then the Boc-protected NH group of the resulting doubly protected derivatives **7a-b**, was alkylated with the appropriate α,ω-dibromoalkane to yield amines **8a-b**. In the following step, all attempts to free the OH group of these derivatives through the cleavage of the silyl ether function with tetrabutylammonium fluoride (TBAF) led to an undesired fluoro/bromo exchange. Finally, deprotection with anhydrous $CeCl_3$ afforded the chlorides **9a-b** presenting a terminal hydroxyl moiety and a suitable leaving group (Cl) for the alkylation of bipyridine. These compounds were reacted in refluxing acetonitrile with the pyridyl pyridinium salt **10**, functionalized with a stoppered C_6 alkyl chain, to afford axles **11a** and **11b** in 65% and 88 % yield, respectively (see Experimental).

In separated experiments, **11a** and **11b** were then suspended in toluene and mixed with an equimolar amount of wheel **Cx**. In these two reactions, no hints of complexation were observed: the heterogeneous mixture never turned homogeneous and the supernatant toluene solution remained uncolored. Heating the two mixtures to reflux for several hours did not change the result. The ESI-MS analysis of the reaction mixtures (carried out in MeOH to provide the solubility of the axle) revealed the presence of the sole unreacted reagents, meaning that no side reaction or reagents degradation took place: in fact, after chromatographic separation, **Cx** was recovered almost quantitatively.

The impossibility to obtain any pseudorotaxane complex through these reactions was mainly ascribed to the bulkiness of the protected secondary amine in **11a** and **11b** that prevent the threading of the axle bearing the carbamate moiety in proximity to the lower rim of the wheel. Overall, the above "threading-and-capping" sequential strategy has shown the remarkable advantages of a complete selectivity in the synthesis of orientational isomers presenting the *N*-station facing the upper rim of the calix[6]arene: **R-UpShort** and **R-UpLong** (Figure 2). On the other hand, its major drawback is the impossibility to obtain assemblies presenting bulky moieties exposed downward or arranged in non-linear conformations, because such dumbbells cannot efficiently thread the wheel component.

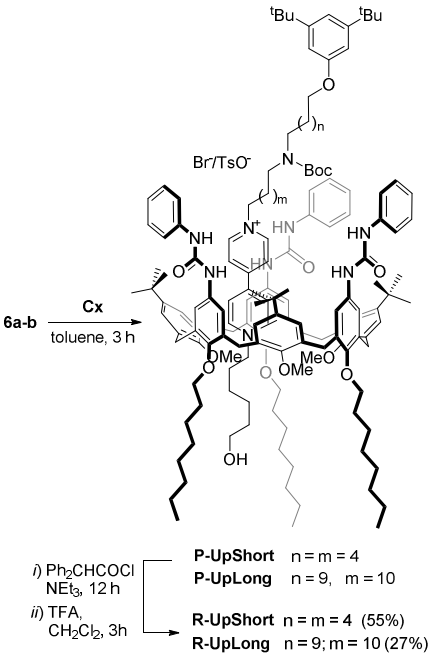

Scheme 2. Synthesis of target rotaxanes **R-UpShort** and **R-UpLong**.

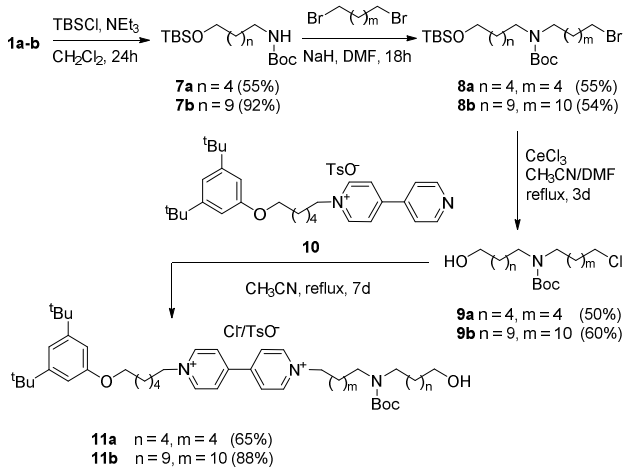

Scheme 3. Synthesis of *N*-Boc protected axles **11a** and **11b.**

To overcome these limitations, we envisaged to investigate whether the recent results we obtained in the supramolecularly-assisted synthesis of oriented calix[6]arene-based rotaxanes[37,38] can be extended to the preparation of rotaxanes that cannot be synthesized with traditional procedures. In this recent work it was indeed shown that the alkylation of pyridyl-pyridinium salts such as **5** and **10** in presence of an analogue of **Cx** takes place preferentially inside the calix[6]arene cavity with the non-alkylated pyridine ring facing the calixarene upper rim. This alkylation gives thus rise to the formation of pseudorotaxane structures. If a bulky terminal group is present on the alkyl chain of the pyridyl-pyridinium guest, the following assisted alkylation and stoppering reactions lead to the formation of oriented rotaxanes, in which the alkyl chain initially appended to the pyridinium, regardless of its length, is located close to the lower rim of the wheel.[37,38]

Starting from these results, we therefore designed the synthesis of the stoppered pyridyl-pyridinium salts having the Boc-protected *N*-station between the phenolic stopper and pyridylpyridinium moiety and alkyl spacers between the amine group and the two opposite endings of different length. In separated experiments, **4a-b** were first reacted with a large excess of 4,4'-bipyridine in refluxing acetonitrile (see scheme 4) and the resulting pyridylpyridinium salts **12a** and **12b**, easily isolated by filtration, were then mixed in toluene with equimolar amounts of **Cx** and **13**. The latter compound is a C_6 alkylating agent mono-stoppered with a bulky diphenylacetic moiety. These supramolecularly-assisted rotaxanation reactions went to completeness after two days of refluxing (solutions turned homogeneous and red-colored). After chromatographic separation, the rotaxanes were immediately treated with TFA in dichloromethane (DCM) to deprotect the *N*-station. After solvent removal, the oriented rotaxanes **R-DownShort** and **R-DownLong** were obtained in 58% and 69% of overall yield. Model compounds dumbbells **DB-Long** and **DB-Short** were synthesized as depicted in Scheme 4.

Rotaxanes Characterization

The inclusion of a bipyridinium-based dumbbell in a calix[6]arene wheel can be assessed through the analysis of the proton chemical shift of some diagnostic signals.[32,33,36,39-41] The presence of a single sharp signal at ca. 3.8 ppm for the lower rim methoxy groups is used to confirm the presence of a single orientational isomer in solution (see Figure 3). Considering the *cone* shape adopted by the calix[6]arene cavity upon threading and its extension due to the three *N*-phenylureas at its upper rim, it is known that all signals of the stoppered alkyl chain facing the phenylureas are more upfield shifted than those belonging to the opposite side chain.[32,33,35,36] To assess the orientation of the asymmetric dumbbell **DB-Short** and **DB-Long** with respect the rims of the wheel, we took advantage of our previous NMR studies carried out on a symmetric rotaxane bearing two C6-alkyl chains at the opposite sides of the bipyridinium station, **R-C6C6** (see Figure 2),[32] which shares with the two-station rotaxanes so far synthesized the same alkylated bipyridinium moiety with a diphenylacetic stopper. In this rotaxane, the methylene group nearby the diphenylacetic stopper, indicated either with the label *1* or *1'* depending on the orientation of its hexyl chain with respect to the asymmetric aromatic cavity (upper and lower rim, respectively, see Figure 2), is greatly affected by changes of the magnetic environment. It gives rise to two well-separated NMR signals at δ = 4.38 and 4.08 ppm (see entry 1, Table 1), with the more upfield-shifted one relative to the methylene group (*1*) of the hexyl chain located toward the wheel upper rim (see Figure 2).[32] Through a simple comparison of the chemical shifts of these signals, it was then possible to foresee that the side chain containing the *N*-station in **R-UpShort** and **R-UpLong** (see Figure 3a-b and Table 1) is oriented toward the wheel upper rim. The same applies for rotaxanes **R-DownShort** and **R-DownLong** where the *N*-station is oriented in the opposite direction (see Figure 3c-d and Table 1). In the two "short" rotaxane isomers **R-UpShort** and **R-DownShort**, characterized by a *N*-containing side chain with short spacers, also the signals of the two methylene groups nearby the ammonium moiety are affected by the orientation of the dumbbell inside **Cx**. In **R-UpShort** these methylene groups resonate as two broad signals at δ = 2.9 and 2.7 ppm, labelled respectively as *#* and *§* (see Figure 3a). In the opposite orientational isomer **R-DownShort** one of these two signals (*§'*) is downfield-shifted at δ = 3.2 ppm (see Figure 3c). In the longer dumbbell of the rotaxane isomers **R-UpLong** and **R-DownLong** both methylene groups give rise to a unique broad signal centered at ca. 2.6 ppm regardless of their position with respect to the cavity. This is coherent with the increased distance of the ammonium group (C_{12} spacer) from the cavity in these two rotaxanes. Moreover, for each rotaxane, 2D NMR measurements (COSY, TOCSY, NOESY, HSQC) were carried out to facilitate the complete characterization of the products. The formation of the two-station rotaxanes was also confirmed by high resolution mass spectrometry (see experimental).

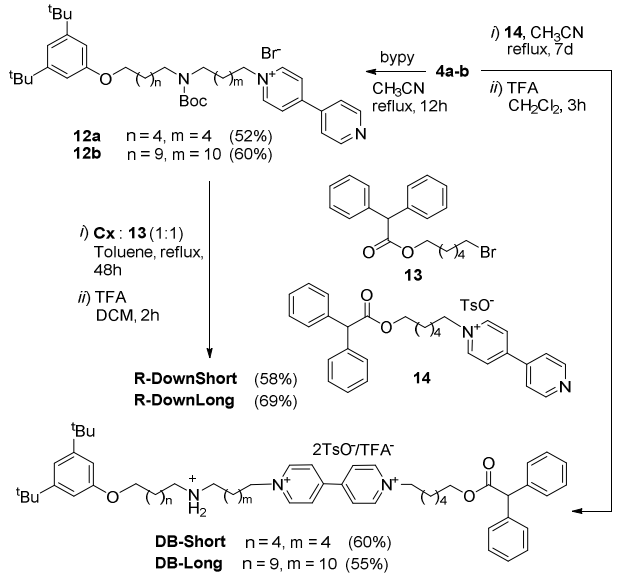

Scheme 4. Supramolecularly assisted synthesis of rotaxanes **R-DownShort** and **R-DownLong** and synthesis of dumbbells **DB-Short** and **DB-Long**.

Table 1 ^{1}H NMR chemical shifts (δ, ppm, C_6D_6, 400 MHz) of the most diagnostic methylene signals of the dumbbell in the series of two-station rotaxanes **R-Down** and **R-Up**. The chemical shift of the same signals for symmetric rotaxane **R-C6C6** were reported for comparison.[a,b]

Rotaxane	Chemical shift (ppm)					
	1'	*1*	*#'*	*#*	*§'*	*§*
R-C6C6	4.38	4.08	/	/	/	/
R-UpShort	4.31	/	/	2.9	/	2.7
R-UpLong	4.32	/	/	2.6	/	2.6
R-DownShort	/	4.03	2.9	/	3.2	/
R-DownLong	/	4.04	2.6	/	2.6	/
DB-Long		4.17			3.0[c]	
DB-Short		4.16			3.0[c]	

[a] For the NMR signals assignment see Figure 3; [b] a primed label indicates the orientation of the methylene group toward the wheel lower rim; [c] in the non-complexed dumbbells these signals are overlapped.

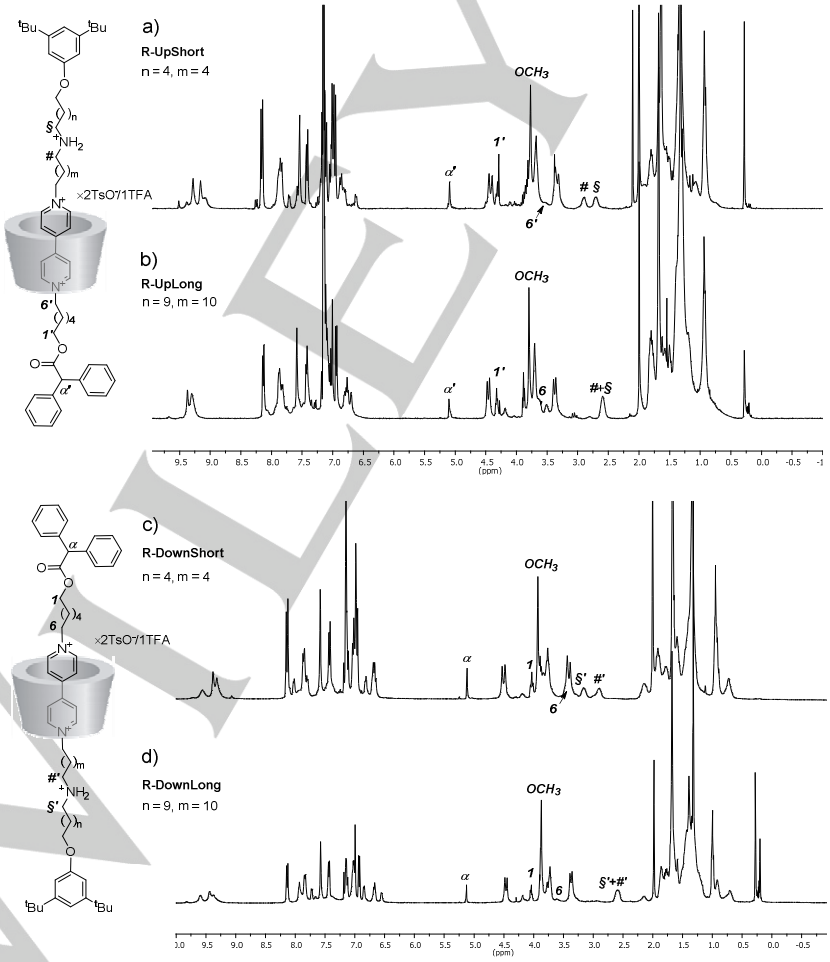

Figure 3. ^{1}H NMR stack plots (C_6D_6, 400 MHz) of the series of two-station rotaxanes (the most diagnostic signals are indicated in sketches on the left).

Rotaxanes Electrochemical Behavior

It is known[34] that parent pseudorotaxanes composed of a bipyridinium-based axle and a trisphenylureido calix[6]arene can be operated by means of electrochemical stimulation, i. e. electrochemical reduction of the bipyridinium unit to its radical cation causes the dethreading of the molecular components. On the other hand, in rotaxanes lacking a second recognition unit for the calixarene the reduction of the bipyridinium ring does not displace the ring from the station.[32,33] The response of the two-station rotaxanes to electrochemical stimulation was steered through Cyclic Voltammetry (CV) and Differential Pulse Voltammetry (DPV) measurements in acetonitrile, and the measured potentials were compared to the ones of non-complexed dumbbells **DB-Long** and **DB-Short** (see Table 2). For sake of comparison, also the reduction potentials of the 1,1'-dioctyl-4,4-bipyridinium (**DOV**) axle and of symmetric rotaxane **R-C6C6** are reported. In line with previously analyzed systems, all compounds show two reversible or quasi-reversible monoelectronic reduction processes.[32] The values of the reduction potentials of the two dumbbells are similar to the ones of **DOV**, thus demonstrating that the electrochemical properties of the bipyridinium moiety are not influenced neither by the stoppers nor by the ammonium units.

As expected, the first reduction potential of each two-station rotaxane isomer is shifted towards more negative values with respect to the corresponding free axle in solution, and falls at almost the same potential as in model compound **R-C6C6** (Figure 4), as a consequence of the stabilization of the bipyridinium unit induced by the calixarene cavity.[32–34] On the other hand, the second reduction potentials are comparable to the ones of non-complexed dumbbells (Figure 4). These results, together with the EPR data (vide infra), indicate that the calixarene ring moves away from the monoreduced bipyridinium unit. Nevertheless, the reversibility of the first reduction waves in the cyclic voltammetry suggests that the shuttling equilibria in the monoreduced state are fast with respect to the scanning speed. The scan rates explored with our apparatus did not evidence any dependence of the peak position and separation on the scan rate, but digital simulations of the experiments and fitting of the experimental data confirmed our hypothesis.

The voltammetric curves obtained on rotaxane **R-UpShort** were fitted according to the scheme reported in Figure 5, by fixing the reduction potentials for the encapsulated and free species to the experimental values. The vertical processes are the electrochemical reactions, whereas the horizontal processes are the shuttling reactions. The values of the thermodynamic constants for these equilibria are also reported. A closer inspection of the reduction potentials (Figure 4) suggests that there is dependence both on the length of the *N*-containing alkyl chains (short or long) and on the position of the ammonium site with respect to the calixarene rims (up or down). The analysis of the second reduction potentials shows that the reduction of the rotaxanes with shorter chains **R-UpShort** and **R-DownShort**, bearing the ammonium unit closer to the macrocycle, is slightly more difficult (regardless of the calix[6]arene orientation) with respect to the reduction of the "long" isomers: this result suggests that a little but non-negligible interaction between the calixarene and the monoreduced bipyridinium is still taking place in the "short" isomers, in agreement with EPR results (vide infra).

Table 2. Electrochemical potentials (vs SCE) of the investigated compounds. Conditions: argon-purged acetonitrile, tetraethylammonium hexafluorophosphate 0.04 M, analyte 300-400 µM.

Species	Reduction potentials (V)	
	E_1	E_2
DOV	-0.42[42]	-0.87[42]
DB-Short	-0.41	-0.85
DB-Long	-0.40	-0.85
R-UpShort	-0.60	-0.94
R-UpLong	-0.61	-0.87
R-DownShort	-0.52	-0.93
R-DownLong	-0.60	-0.88
R-C6C6	-0.64[32,33]	-1.15[32,33]

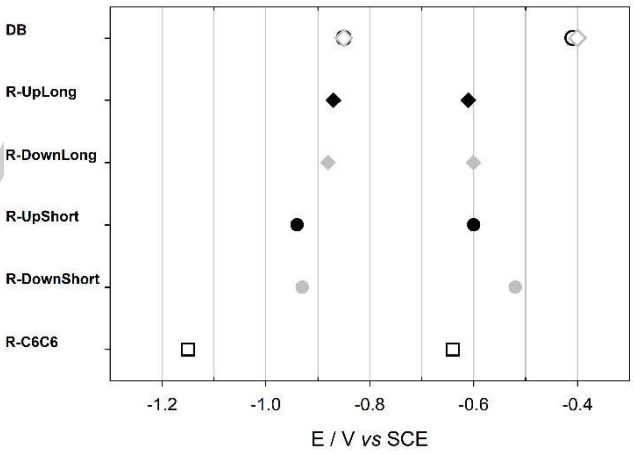

Figure 4. Genetic diagram of the measured reduction potentials of the studied compounds: dumbbells **DB-Short** (empty circles) and **DB-Long** (empty diamonds), two-stations rotaxanes **R-UpLong** (black diamonds), **R-DownLong** (grey diamonds), **R-UpShort** (black circles), **R-DownShort** (grey circles), and one-station rotaxane **R-C6C6** (empty squares).

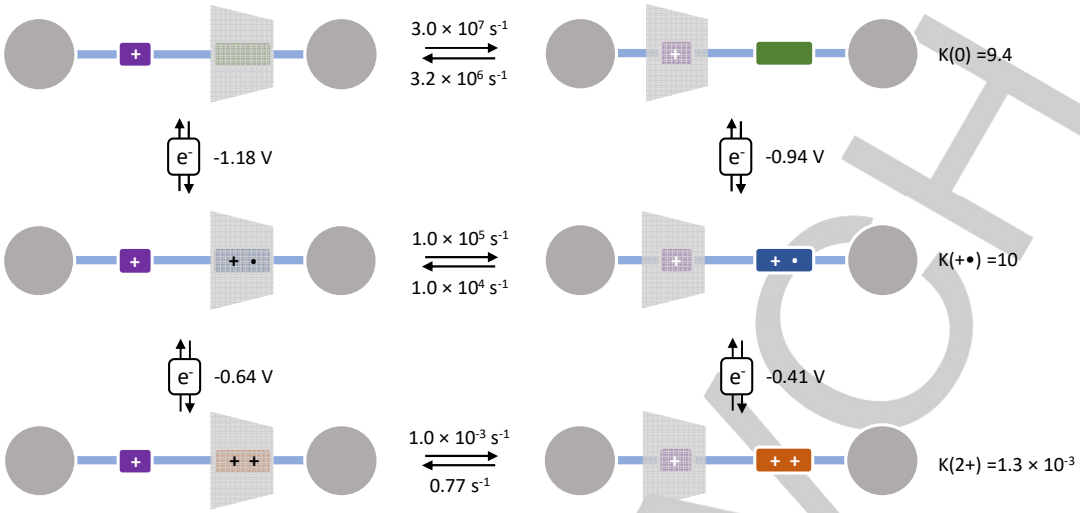

Figure 5. Reaction scheme reporting the thermodynamic and kinetic data for the simulated voltammogram of **R-UpShort**. Reduction potentials partly taken from refs. [32] and [33].

This finding would also suggest that when the ammonium is close to the bipyridinium unit, it is possible for the calixarene macrocycle to interact with both sites simultaneously, regardless of the orientation of the axle. This observation is somehow surprising, because the two rims of the calix[6]arene are different from a chemical point of view and it is therefore not easy to imagine different interaction modes that result in very similar interaction energies. The analysis of the first reduction potential enlightens also a dependence on the relative orientation of the axle and the ring. Rotaxane **R-DownShort**, with a short *N*-containing chain close to the lower rim of the calixarene, is easier to reduce with respect to all the other rotaxanes. This would suggest that the calixarene is less engaged in charge transfer interactions with the bipyridinium unit, possibly because involved in the interaction with the ammonium site already in the oxidized form, besides in the monoreduced state as suggested by EPR data (vide infra). This hypothesis is also supported by the reversed position of the NMR signals of **R-DownShort** and **R-UpShort** (vide supra).

Rotaxanes EPR Measurements

The hypothesis of a shuttling motion of **Cx** was also supported by the EPR spectra of non-complexed dumbbells and rotaxanes recorded after electrochemical reduction in deoxygenated acetonitrile at room temperature. The EPR spectra of the bipyridinium radical cations, bpy(+•), obtained by one-electron reduction are reported in Figure 6. According to previous studies on the radical cation of 1,1'-dialkyl-4,4'-bipyridinium derivatives,[33] all the spectra can be well reproduced by assuming the coupling of the unpaired electron with two equivalent N atoms and three groups of four equivalent protons: one group is due to the methylene groups of the two chains and the other two equivalent sets arise from the aromatic protons. By using the above spectral pattern all the spectra can be nicely reproduced with the hyperfine splitting constants reported in Table 3. In all cases, the g-factors were found to be close to 2.0031. According to the literature,[33] the smaller hyperfine coupling constant for H atoms was assigned to the aromatic α-protons, whereas the larger coupling was attributed to the methylene groups of the two alkyl chains. Inspection of these data clearly shows that: *i*) EPR parameters of the mono-reduced double-station rotaxanes are similar to those measured for the non-complexed mono-reduced dumbbells **DB-Short**(+•) and **DB-Long**(+•) (Figure 6); *ii*) the values of the hyperfine coupling constants are consistent with a symmetric distribution of the two aromatic rings of the bipyridine. We have already shown[33] that trapping bpy(+•) in the asymmetric wheel of **Cx** induces a non-symmetric distribution of the spin density in the two heterocyclic rings. Thus, present results suggest that bpy(+•) does not interact significantly with the calix[6]arene cavity in all derivatives, irrespective of the length of the alkyl chains on the axle and the relative position of the two components of the rotaxane.

Table 3. EPR hyperfine splitting constants (*a*, in Gauss) of radical cations obtained after electrochemical reduction of the bipyridinium unit at room temperature in CH_3CN.

	a_{2N}	a_{2CH_2}	a_{4H_β}	a_{4H_α}
DB-Short(+•)	4.10	4.06	1.61	1.11
DB-Long(+•)	4.13	4.05	1.58	1.12
R-UpShort(+•)	4.16	3.98	1.66	1.20
R-DownShort(+•)	4.17	4.11	1.47	1.30
R-UpLong(+•)	4.13	4.01	1.62	1.17
R-DownLong(+•)	4.14	4.04	1.61	1.15

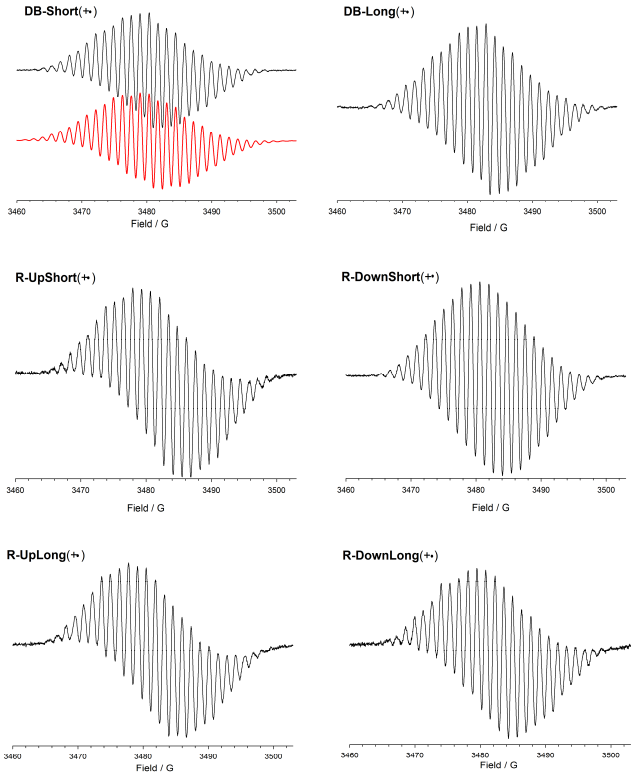

Figure 6. EPR spectra (recorded in acetonitrile) of electrochemically reduced non-complexed dumbbells and two-station rotaxanes.

The hyperfine splitting constants measured in the EPR spectrum of the "short" rotaxanes R-UpShort(+•) and R-DownShort(+•) which are slightly different with respect to those measured with the non-complexed dumbbells and "long" rotaxanes radical cations deserve a brief comment. Actually, these small differences suggest that it is possible for the aromatic or aliphatic tails of the calix[6]arene to maintain a little but non-negligible interaction with the monoreduced bipyridinium unit when the ammonium recognition site is close to the bipyridinium unit. In conclusion, EPR results, in agreement with the electrochemical data, confirm that the addition of one electron on the bipyridinium site induces the displacement of the wheel away from it.

Conclusions

In this paper, the design, the synthesis and the structural characterization of new oriented double-station calix[6]arene-based rotaxanes were presented. Several challenges in the field of calixarene-based molecular machines have been tackled. First, two different synthetic procedures have been followed for the synthesis of the two orientational isomers. The up isomers, bearing an ammonium station in proximity to the upper rim of the wheel, were synthesized following a traditional sequential threading-and-capping procedure; the down isomers, in which the second recognition unit faces the lower part of the wheel, were obtained exploiting a supramolecularly assisted strategy which was recently reported.[37,38] Moreover, we have demonstrated that the ammonium moiety can play the role of a secondary station for the calixarene and the ability of these systems to behave as molecular shuttles driven by electrochemical stimulation. Voltammetric and EPR measurements evidenced that, upon the first monoelectronic reduction of the axle's bipyridinium unit, a rearrangement of the systems takes place. This indicates that, coherently with our initial hypothesis, the electrochemical input induces the shuttling of the calixarene towards the more favored second recognition site and the complete reduction of the radical cation to its neutral form takes place outside the calixarene cavity. Finally, we have observed a dependence of the shuttling both on the length of the chain of the axles and on the relative orientation of the molecular components. On the basis of the collected data, in a symmetric rotaxane bearing a central bipyridinium unit and two peripheral ammonium stations connected by short spacers, reduction of the electroactive unit is expected to induce the shuttling of the calixarene preferentially towards the ammonium station located at its lower rim, i.e. a directional motion would be dictated only by the orientation of the wheel onto a symmetric axle. Three-stations rotaxanes based on these architectures are currently under investigation in our laboratories.

Experimental Section

Synthesis: Toluene, THF, acetonitrile and dichloromethane were dried by following standard procedures, other reagents were of reagent grade quality, obtained from commercial sources and used without further purification. Chemical shifts are expressed in ppm using the residual solvent signal as internal reference. Mass spectra were determined in ESI mode. Compounds **1a**,[43] **1b**,[44] **2a**,[43] **7a**,[45] **13**,[35] **5**,[43] **10**,[46] **14**,[33] **R-C6C6**,[32] axle **DOV**,[34] and wheel **Cx**[47] were synthesized according to reported procedures.

***Tert*-butyl-*N*-{11-[(4-methylbenzenesulfonyl)oxy]undecyl}carbamate (2b):** to a solution of **1b** (3.5 g, 12.2 mmol) in dry dichloromethane (50 mL), triethylamine (1.7 g, 17.9 mmol), tosyl chloride (3 g, 15.8 mmol) and a catalytic amount of DMAP were added in this order. After stirring at room temperature for 24h, the reaction was quenched with water (50 mL). The separated organic phase was dried over anhydrous $CaCl_2$, filtered and the solvent was evaporated to dryness under reduced pressure. The sticky residue was purified by column chromatography (*n*-hexane/ethyl acetate 85:15) to afford **2b** as a white solid (75%); mp 57-59 °C; ^{1}H NMR (400 MHz, $CDCl_3$, δ): 1.2–1.4 (m, 14H), 1.47 and 1.4–1.5 (s, m, 11H), 1.6–1.7 (m, 2H), 2.47 (s, 3H), 3.11 (br. s, 2H), 4.04 (t, *J* = 6.5 Hz, 2H), 4.5 (br. s, 1H), 7.36 (d, *J* = 7.6 Hz, 2H), 7.81 (d, *J* = 7.6 Hz, 2H); ^{13}C NMR (100 MHz, $CDCl_3$, δ): 21.6, 25.3, 26.8, 28.4, 28.8, 28.9, 29.2, 29.3 (2 res.), 29.4, 30.0, 40.6, 70.7, 78.8, 127.8, 129.8, 133.2, 144.6, 156.2 ppm; ESI-MS(+) m/z (%) [ion]: 464 (100) $[M+Na]^+$. Anal. Calcd for $C_{23}H_{39}NO_5S$: C, 62.55; H, 8.90; N, 3.17. Found: C, 62.61.43; H, 8.95; N, 2.99%.

General procedure for the synthesis of 3a-b: to a solution of 3,5-di-*tert*-butylphenol (6.3 mmol) and K_2CO_3 (2.6 g, 18.8 mmol) in dry DMF (50 mL), tosylate (**2a** or **2b**, 7 mmol) was added. The resulting reaction mixture was stirred at 80 °C for 12h. After cooling at room temperature,

the reaction was quenched with water (50 mL) and extracted with ethyl acetate (3 × 100 mL). The separated organic phase was dried over Na_2SO_4 and evaporated to dryness under reduced pressure.

***Tert*-butyl *N*-[6-(3,5-di-*tert*-butylphenoxy)hexyl]carbamate (3a):** the residue was purified by column chromatography (*n*-hexane/acetone 85:15) to afford **3a** as a colorless oil (53%); ^{1}H NMR (400 MHz, $CDCl_3$, δ): 1.33 (s, 18H), 1.4–1.6 and 1.47 (2m, s, 15H), 1.8–1.9 (m, 2H), 3.14 (t, *J* = 6.7 Hz, 2H), 3.98 (t, *J* = 6.4 Hz, 2H), 4.5 (br. s, 1H), 6.77 (s, 2H), 7.03 (s, 1H); ^{13}C NMR (100 MHz, $CDCl_3$, δ): 25.9, 26.6, 28.5, 29.4, 30.1, 31.5, 35.0, 40.6, 67.5, 77.2, 108.8, 114.8, 152.1, 156.0, 158.6 ppm; ESI-MS(+) m/z (%) [ion]: 428 (100) $[M+Na]^+$.

***Tert*-butyl *N*-[11-(3,5-di-*tert*-butylphenoxy)undecyl]carbamate (3b):** the residue was purified by column chromatography (*n*-hexane/THF 85:15) to afford **3b** as a colorless oil (43%); (400 MHz, $CDCl_3$, δ): 1.2–1.4 and 1.33 (m, s, 30H), 1.4–1.5 (m, 13H), 1.8–1.9 (m, 2H), 3.12 (t, *J* = 6.4 Hz, 2H), 3.98 (t, *J* = 6.4 Hz, 2H), 4.51 (br. s, 1H), 6.78 (s, 2H), 7.03 (s, 1H); ^{13}C NMR (75 MHz, $CDCl_3$, δ): 26.1, 26.8, 28.4, 29.3, 29.5 (3 res.), 29.6, 30.1, 30.3, 31.5, 35.0, 40.6, 72.9, 79.1, 108.8, 114.7, 152.1, 156.0, 158.7 ppm; ESI-MS(+) m/z (%) [ion]: 499 (100) $[M+Na]^+$.

General procedure for the synthesis of 4a-b: to a solution of the proper *N*-protected amine (**3a** or **3b**, 2.5 mmol) in dry DMF (50 mL), kept under inert atmosphere and cooled at 0 °C through an external ice bath, NaH (0.2 g of a 60% dispersion in mineral oil, ca. 5 mmol) was slowly added. The resulting reaction mixture was stirred at room temperature for 3 h, then cooled again at 0 °C and the properα,ω-dibromoalkane (7.5 mmol) was added dropwise. After stirring for 18 h at room temperature, the reaction was carefully quenched with water (40 mL) and extracted with ethyl acetate (3 × 50 mL). The organic phase was dried over Na_2SO_4 and evaporated under reduced pressure.

***Tert*-butyl *N*-(6-bromohexyl)-*N*-[6-(3,5-di-*tert*-butylphenoxy)hexyl] carbamate (4a):** the residue was purified by column chromatography (*n*-hexane/THF 95:5) to afford **4a** as a colorless oil (0.75 g, 57%); ^{1}H NMR (400 MHz, $CDCl_3$, δ): 1.33 (s, 18H) 1.4–1.6 and 1.48 (m, s, 21H), 1.8–1.9 (m, 4H), 3.1–3.2 (m, 4H), 3.42 (t, *J* = 6.8 Hz, 2H), 3.98 (t, *J* = 6.4 Hz, 2H), 6.77 (d, *J* = 1.6 Hz, 2H), 7.03 (t, *J* = 1.6 Hz, 1H); ^{13}C NMR (100 MHz, $CDCl_3$, δ): 26.0, 26.1, 26.7, 28.0, 28.5, 30.0, 31.5, 32.8, 33.8, 35.0, 46.9, 47.0, 67.6, 79.0, 108.8, 114.8, 152.1, 155.6, 158.6 ppm; ESI-MS(+) m/z (%) [ion]: 590 (95), 591 (25), 592 (100) $[M+Na]^+$.

***Tert*-butyl *N*-(12-bromododecyl)-*N*-[11-(3,5-di-*tert*-butylphenoxy)undecyl] carbamate (4b):** the residue was purified by column chromatography (n-hexane/THF 95:5) to afford **4b** as a colorless oil (1.35 g, 58%).^{1}H NMR (400 MHz, $CDCl_3$, δ): 1.2–1.4 and 1.34 (m, s, 44H), 1.4–1.5 (m, 17H), 1.8–1.9 (2m, 4H), 3.2 (br. s, 4H), 3.43 (t, *J* = 6.8 Hz, 2H), 3.98 (t, *J* = 6.5 Hz, 2H), 6.78 (d, *J* = 1.6 Hz, 2H), 7.03 (t, *J* = 1.6 Hz, 1H); ^{13}C NMR (100 MHz, $CDCl_3$, δ): 26.2, 26.9, 28.2, 28.5, 28.8, 29.4 (3 res.), 29.5 (4 res.), 29.6 (5 res.), 29.6, 30.4, 31.5, 32.9, 34.1, 35.0, 47.1, 67.8, 78.9, 108.8, 114.8, 152.1, 155.7, 158.7 ppm; ESI-MS(+) m/z (%) [ion]: 744 (90), 745 (40), 746 (98), 747 (45) $[M+Na]^+$.

General procedure for the synthesis of axles 6a-6b: in a sealed glass autoclave, a solution of salt **5** (0.14 g, 0.3 mmol) and of the proper bromide (**4a** or **4b**, 0.6 mmol) in 5 mL of dry acetonitrile was refluxed for 7 days. After cooling to room temperature, the reaction mixture was refrigerated at 0 °C until precipitation of a yellow solid was observed.

Axle 6a: the yellow precipitate was collected by Buchner filtration and washed with cold acetonitrile (46%); mp = 197-198 °C; ^{1}H NMR (300 MHz, CD_3OD, δ): 1.33 (s, 18H), 1.4–1.7 and 1.48 (m, s, 25H), 1.7–1.9 (m, 2H), 2.0–2.2 (m, 4H), 2.39 (s, 3H), 3.24 (t, *J* = 6.8 Hz, 4H), 3.60 (t, *J* = 6.2 Hz, 2H), 4.00 (t, *J* = 6.2 Hz, 2H), 4.78 (t, *J* = 7.5 Hz, 4H), 6.77 (s, 2H), 7.05 (s, 1H), 7.25 (d, *J* = 8 Hz, 2H), 7.70 (d, *J* = 8 Hz, 2H), 8.71 (d, *J* = 6.5 Hz, 4H), 9.30 (d, *J* = 6.5 Hz, 4H); ^{13}C NMR (75 MHz, CD_3OD, δ): 18.0, 23.8, 23.9, 24.1, 24.2, 24.4, 24.8, 26.0, 26.8, 27.2, 27.4, 27.7, 29.1, 29.6, 30.4, 32.9, 46.2, 59.8, 60.3, 65.8, 77.8, 107.1, 112.8, 124.1, 125.4, 127.1, 138.8, 140.9, 145.4, 148.3, 150.3, 154.5, 157.3 ppm; ESI-MS(+) m/z (%) [ion]: 744.5 (100) $[M-H]^+$; Anal. Calcd for $C_{54}H_{82}BrN_3O_7S$: C, 65.04; H, 8.29; N, 4.21. Found: C, 64.22.43; H, 7.99; N, 4.42%.

Axle 6b: the yellow precipitate was collected by Buchner filtration and washed with cold acetonitrile (50%); mp > 300 °C dec.; ^{1}H NMR (400 MHz, CD_3OD, δ): 1.2–1.4 (m, 44H), 1.4–1.6 (m, 21H), 1.7–1.9 (m, 4H), 2.0–2.2 (m, 4H), 2.38 (s, 3H), 3.18 (t, *J* = 7.2 Hz, 4H), 3.58 (t, *J* = 6.4 Hz, 2H), 3.97 (t, *J* = 6.4 Hz, 2H), 4.76 (m, 4H), 6.74 (s, 2H), 7.02 (s, 1H), 7.24 (d, *J* = 8 Hz, 2H), 7.69 (d, *J* = 8 Hz, 2H), 8.69 (d, *J* = 6.4 Hz, 4H), 9.29 (d, *J* =6.4 Hz, 2H); ^{13}C NMR (100 MHz, CD_3OD, δ): 20.0, 25.0, 25.6, 25.9 (2 res.), 26.5, 26.6, 27.5 (2 res.), 27.8 (2 res.), 28.3, 28.5, 28.8, 29.1, 29.2 (2 res.), 29.3, 29.4, 30.6, 31.1, 31.2, 31.8, 32.6, 33.1 (2 res.), 34.4, 46.7, 61.2, 61.8, 67.4, 79.2, 108.6, 114.3, 125.5, 126.9, 128.5, 140.3, 142.3, 145.7, 149.8, 151.7, 156.0, 158.8 ppm; ESI-MS(+) m/z (%) [ion]: 899.8 (100), 900.7 (65) $[M-H]^+$; 1070.6 (25), 1071.8 (20) $[M+TsO]^+$; Anal. Calcd for $C_{65}H_{104}BrN_3O_7S$: C, 67.80; H, 9.10; N, 3.65. Found: C, 66.95; H, 8.65; N, 4.01%.

General procedure for the sequential synthesis of two-station rotaxanes R-UpShort and R-UpLong: the proper mono-stoppered axle (**6a** or **6b**, 0.06 mmol) was suspended in a solution of wheel **Cx** (0.09 g, 0.06 mmol) in anhydrous toluene (15 mL). The suspension was stirred at room temperature for 3 hours until the solution turned homogeneous and dark-red colored. Triethylamine (0.01 g, 0.1 mmol) and diphenylacetyl chloride (0.03 g, 0.1 mmol) were then added, and the resulting reaction mixture was stirred overnight at room temperature. After removing the solvent under reduced pressure, the solid residue was portioned between dichloromethane and water. The organic phase was separated and evaporated under reduced pressure, and crude product was purified by column chromatography (dichloromethane/methanol 50:1). The resulting protected (*N*-Boc) rotaxane was then dissolved in 10 mL of anhydrous dichloromethane and 2 mL of trifluoroacetic acid were added dropwise. The solution turned yellow. After stirring at room temperature for 2 hours, the solvent was evaporated under reduced pressure to afford the desired deprotected rotaxane.

R-UpShort: the product was isolated as a red solid (55%); mp > 300 °C dec.; ^{1}H NMR (400 MHz, C_6D_6, δ): 0.8 (br. s, 2H), 0.8–1.0 (m, 17H), 1.1 (br. s, 6H), 1.2–1.4 and 1.33 (br. s, s, 68H), 1.5–1.7 and 1.64 (br. s, s, 46H), 1.8 (br. s, 12H), 1.9 (br. s, 2H), 2.00 (s, 12H), 2.10 (s, 4H), 2.7 (br. s, 2H), 2.9 (br. s, 2H), 3.2–3.4 (m, 8H), 3.5–3.7 (2 br. s, 12H), 3.7–3.9 and 3.77 (m, s, 12H), 4.31 (t, *J* = 6.0 Hz, 2H), 4.42 (d, *J* = 12.0 Hz, 6H), 5.09 (s, 1 H), 6.59 (d, *J* =5.2 Hz, 2H), 6.7 (br. s, 2H), 6.9 (br. s, 3H), 7.0 (br. s., 14H), 7.2 (br. s, 11H), 7.42 (d, *J* = 7.2 Hz, 4H), 7.54 (s, 6H), 7.70 (d, *J* = 5.2 Hz, 2H), 7.83 (d, *J* = 6.8 Hz, 6H), 8.2 (br. s, 2H), 8.23 (d, *J* = 8.0 Hz, 4H), 9.0-9.3 (m, 7H); ^{13}C NMR (100 MHz, C_6D_6, δ): 13.2, 20.0, 21.9, 24.6, 25.0, 25.2, 25.6, 25.7, 26.2, 27.1, 27.2, 28.3, 28.7, 28.8, 28.9, 29.9, 30.7, 31.1, 33.8, 33.9, 47.9, 48.2, 56.4, 59.8, 59.9, 60.3, 61.1, 62.8, 64.0, 66.5, 72.3, 108.3, 113.6, 115.8, 117.3, 120.4, 124.0, 124.8, 125.1, 125.7, 126.4, 126.7, 127.0, 127.3, 127.7 (2 res) 127.8, 128.0, 128.5, 128.6, 131.2, 132.8, 136.5, 138.2, 138.6, 140.3, 142.1, 142.5, 143.5, 145.3, 147.5, 151.1, 152.0, 152.5, 158.6, 171.1 ppm; HRMS (*m/z*): $[M]^{2+}$ calcd for $C_{158}H_{209}N_9O_{12}$, 1212.3005; found, 1212.3027.

R-UpLong: the product was isolated as a red solid (27%); mp > 300 °C dec.; ^{1}H NMR (400 MHz, C_6D_6, δ): 0.6–1.0 (m, 9H), 1.1–1.3 (m, 57H), 1.4–1.6 (m, 12H), 1.69 (s, 18H), 1.8 (br. s, 4H), 1.99 (s, 6H), 2.59 (br. s,

4H), 3.38 (d, *J* = 14.4 Hz, 6H), 3.5 (br. s, 4H), 3.7 (br. s, 6H), 3.79 (s, 9H), 3.88 (t, *J* = 7.0 Hz, 2H), 4.32 (t, *J* = 6.8 Hz, 2H), 4.46 (d, *J* =14.4 Hz, 6H), 5.11 (s, 1H), 6.9 (d, *J* = 5.2 Hz, 2H), 6.77 (t, *J* = 6.8 Hz, 3H), 6.83 (d, *J* = 5.2 Hz, 2H), 6.94 (d, *J* = 8.0 Hz, 4H), 7.0 (m, 4H), 7.15 (m, 7H), 7.43 (m, 4H), 7.59 (s, 6H), 7.82 (s, 6H), 7.88 (d, *J* = 5.2 Hz, 2H), 8.14 (d, *J* = 8.0 Hz, 4H), 9.2-9.4 (m, 7H); ^{13}C NMR (100 MHz, C_6D_6, δ): 14.0, 20.8, 22.8, 25.7 (2 res.), 25.8 (2 res.), 26.1 (2 res.), 26.4, 26.5, 26.6 (2 res.), 26.7, 28.8, 29.1, 29.2, 29.5 (2 res.), 29.6, 29.7 (2 res.), 29.8 (2 res.), 30.7, 30.8, 31.3, 31.5, 31.6, 31.9, 32.0 (2 res.), 34.6, 34.7, 38.2, 47.4, 47.5, 57.2, 59.7, 60.8, 64.8, 67.5, 73.1, 109.2, 114.4, 116.6, 118.1, 121.2. 124.8, 125.6, 126.4, 127.2, 128.3, 128.4, 128.5, 128.6, 128.7, 128.8, 129.3, 131.7, 132.0, 133.6, 137.3, 139.0, 139.6, 141.2, 142.9, 143.1, 144.1, 148.2, 148.4, 151.9, 152.9, 153.3, 159.5 ppm; HRMS (*m/z*): $[M]^{2+}$ calcd for $C_{169}H_{231}N_9O_{12}$, 1289.3866; found, 1289.3859.

***Tert*-butyl *N*-{11-[(*tert*-butyldimethylsilyl)oxy]undecyl} carbamate (7b):** *Tert*-butyl-chlorodimethylsilane (0.89 g, 5.9 mmol) was slowly added to a solution of **1b** (1.4 g, 5 mmol) and triethylamine (0.6 g, 6 mmol) in dry dichloromethane (100 mL). A catalytic amount of DMAP was added. After stirring at room temperature for 2 hours, the reaction was quenched with water (50 mL) and the organic phase was separated, washed with brine, dried over anhydrous $CaCl_2$ and filtered. The solvent was removed under reduced pressure to afford **7b** as a colorless oily residue (92%). ^{1}H NMR (400 MHz, $CDCl_3$, δ): 0.05 (s, 6H), 0.90 (s, 9H), 1.3–1.5 (m, 14H), 1.4–1.5 (m, 13 H), 3.1 (br. s, 2H), 3.60 (t, *J* = 6.8 Hz, 2H), 4.5 (br. s, 1H); ^{13}C NMR (100 MHz, $CDCl_3$, δ): –5.3, 14.1, 18.4, 22.6, 25.7, 25.8, 26.0, 26.8, 28.4, 29.3, 29.4, 29.5 (2 res.), 29.6, 30.1, 31.6, 32.9, 40.7, 63.3, 78.9, 156.0 ppm; ESI-MS(+) m/z (%) [ion]: 424 (100), 425 (30) $[M+Na]^+$.

General procedure for the synthesis of 8a-b: to a solution of the proper *N*-protected amine (**5a** or **5b**, 4.4 mmol) in dry DMF (50 mL), kept under inert atmosphere and cooled at 0 °C through an external ice bath, NaH (0.35 g of a 60% dispersion in mineral oil, ca. 9 mmol) was slowly added. The resulting reaction mixture was stirred at room temperature for 3 h, and then cooled again at 0 °C and the proper α,ω-dibromoalkane (17.4 mmol) was added dropwise. After stirring for 24 h at room temperature, the reaction was carefully quenched with water (100 mL) and extracted with ethyl acetate (3 × 50 mL). The organic phase was dried over Na_2SO_4 and evaporated under reduced pressure.

***Tert*-butyl *N*-(6-bromohexyl)-*N*-{6-[(tert-butyldimethylsilyl)oxy]hexyl} carbamate (8a):** the residue was purified by column chromatography (*n*-hexane/THF 9:1) to afford **8a** as a colorless oil (1.19 g, 55%). ^{1}H NMR (400 MHz, $CDCl_3$, δ): 0.009 (s, 6H), 0.86 (s, 9H), 1.2–1.3 (m, 4H), 1.42 (s, 9H), 1.4–1.5 (m, 10 H), 1.8–1.9 (m, 2H), 3.1 (br. s, 4H), 3.36 (t, *J* =7 Hz, 2H), 3.56 (t, *J* = 8 Hz, 2H); ^{13}C NMR (100 MHz, $CDCl_3$, δ): –5.26, 14.1, 18.4, 22.7, 25.6, 25.9, 26.1, 26.7, 28.0, 29.7,30.3, 32.8, 33.8, 46.8, 47.0, 63.2, 79.0, 155.6 ppm; ESI-MS(+) m/z (%) [ion]: 516 (100), 518 (97), 519 (30) $[M+Na]^+$.

***Tert*-butyl *N*-(12-bromododecyl)-*N*-{11-[(tert-butyldimethylsilyl)oxy]undecyl} carbamate (8b):** the residue was purified by column chromatography (*n*-hexane/THF 98:2) to afford **8b** as a colorless oil (2.52 g, 54%). ^{1}H NMR (300 MHz, $CDCl_3$, δ): 0.06 (s, 6H), 0.91 (s, 9H), 1.2–1.3 (m, 28H), 1.46 (s, 9H), 1.4–1.6 (m, 8H), 1.8–1.9 (m, 2H), 3.15 (t, *J* = 7 Hz, 4H), 3.42 (t, *J* = 6.8 Hz, 2H), 3.61 (t, *J* = 6.6 Hz, 2H); ^{13}C NMR (100 MHz, $CDCl_3$, δ): –5.3, 25.8, 26.0, 26.9, 28.2, 28.5, 28.8, 29.4, 29.5, 29.6, 32.8, 32.9, 34.0, 47.0, 63.3, 78.8, 155.6 ppm; ESI-MS(+) m/z (%) [ion]: 648 (95), 650 (100), 651 (40) $[M+H]^+$.

General procedure for the synthesis of 9a-b: to a solution of the proper bromide **8a** or **8b** (1.6 mmol) in a mixture of dry acetonitrile (80 mL) and DMF (10 mL), anhydrous cerium(III) chloride (3.1 mmol) was added. The reaction mixture was refluxed for 3 days. The solution was then cooled at room temperature and the solvent removed under reduced pressure. The oily residue was taken up with ethyl acetate (100 mL) and washed with water (3 × 50 mL). The separated organic phase was dried over Na_2SO_4 and evaporated under reduced pressure.

***Tert*-butyl *N*-(6-chlorohexyl)-*N*-(6-hydroxyhexyl) carbamate (9a):** the crude product was purified by column chromatography (*n*-hexane/THF 6:4) to afford chlorinated product **9a** as a colorless oil (50%). ^{1}H NMR (400 MHz, $CDCl_3$, δ): 1.3–1.4 (m, 4H), 1.47 (s, 9H), 1.4–1.6 (m, 8H), 1.6 (br. s, 2H), 1.8–1.9 (m, 2H), 3.2 (br. s, 4H), 3.55 (t, *J* = 6.4 Hz, 2H), 3.65 (t, *J* = 6 Hz, 2H); ^{13}C NMR (100 MHz, $CDCl_3$, δ): 26.2, 26.7, 28.5, 31.0, 32.6, 32.7, 45.0, 46.8, 62.6, 62.9, 79.1, 155.7 ppm; ESI-MS(+) m/z (%) [ion]: 336 (100), 338 (30), 337 (20) $[M+H]^+$; 358 (100), 360 (30) 359 (20) $[M+Na]^+$; 374 (100), 376 (30), 375 (20) $[M+K]^+$.

***Tert*-butyl *N*-(12-chlorododecyl)-*N*-(11-hydroxyundecyl) carbamate (9b):** the crude product was purified by column chromatography (*n*-hexane/ethyl acetate 9:1) to afford **9b** as a colorless oil (0.22 g, 60%). ^{1}H NMR (400 MHz, $CDCl_3$, δ) 1.2–1.3 (m, 28H), 1.45 (s, 9H), 1.4–1.6 (m, 8H), 1.7–1.8 (m, 2H), 3.13 (br. s, 4H), 3.53 (t, *J* = 6.8 Hz, 2H), 3.63 (t, *J* = 6.8 Hz, 2H); ^{13}C NMR (100 MHz, $CDCl_3$, δ): 25.7, 26.9, 28.5, 28.9, 29.4 (2 res.), 29.5 (3 res.), 29.6, 32.6, 32.8, 45.1, 47.0, 63.0, 78.9, 155.7 ppm; ESI-MS(+) m/z (%) [ion]: 490 (100), 491 (30), 492 (30) $[M+H^+]$; 512 (100), 513 (30), 514 (30) $[M+Na^+]$; 528 (100), 529 (30), 530 (20) $[M+K]^+$.

General procedure for the synthesis of axles 11a and 11b: 10 (0.092 g, 0.15 mmol) and the proper chloride **9a** or **9b** (0.3 mmol) were dissolved in 5 mL of dry acetonitrile and placed in a glass autoclave. After sealing the autoclave under inert atmosphere, the resulting reaction mixture was refluxed under stirring for 7 days. After this period, the reaction mixture was cooled to room temperature, diluted with 10 mL of ethyl acetate and then placed in a refrigerator at 0 °C to promote the precipitation of the desired axle.

Axle 11a: a sticky white solid was collected by Buchner filtration and washed with cold ethyl acetate (65%). ^{1}H NMR (400 MHz, CD_3OD, δ): 1.3–1.6 (m, 36H), 1.83 (t, *J* = 6.8 Hz, 2H), 2.14 (t, *J* = 7.2 Hz, 4H), 2.37 (s, 6H), 3.1–3.2 (m, 4H), 3.5–3.6 (m, 2H), 3.99 (t, *J* = 6.0 Hz, 2H), 4.76 (t, *J* = 7.2 Hz, 4H), 6.74 (s, 2H), 7.03 (s, 1H), 7.24 (d, *J* = 8 Hz, 4H), 7.70 (d, *J* =8 Hz, 4H), 8.66 (d, *J* = 6.0 Hz, 4H), 9.27 (d, *J* = 6.0 Hz, 4H); ^{13}C NMR (100 MHz, CD_3OD, δ) 19.9, 25.3, 25.6, 26.3, 27.4, 28.9, 30.5, 31.1, 32.2, 34.4, 61.2, 61.4, 61.8, 67.0, 79.3, 108.5, 114.4, 125.6, 126.9, 128.5, 140.3, 145.7, 149.9, 151.9, 156.0, 158.7, 160.7 ppm; ESI-MS(+) m/z (%) [ion]: 745 (100), 746 (50), 747 (20) $[M-H]^+$; Anal. Calcd for $C_{54}H_{82}ClN_3O_7S$: C, 68.07; H, 8.68; N, 4.41. Found: C, 67.91; H, 8.32; N, 4.05%.

Axle 11b: a sticky yellow solid was collected by Buchner filtration (88%). ^{1}H NMR (400 MHz, CD_3OD, δ): 1.3–1.6 (m, 67H), 1.8–1.9 (m, 2H), 2.1–2.2 (m, 4H), 2.39 (s, 3 H), 3.19 (t, *J* = 7.6 Hz), 3.55 (t, *J* = 6.8 Hz, 2H), 4.00 (t, *J* = 6.4 Hz, 2H), 4.8 (m, 4H), 6.75 (s, 2H), 7.02 (s, 1H), 7.25 (d, *J* = 8 Hz, 2H), 7.72 (d, *J* =8 Hz, 2H), 8.71 (d, *J* = 6.4 Hz, 4H), 9.3 (m, 4H); ^{13}C NMR (100 MHz, CD_3OD, δ): 25.6, 25.9, 26.5 (2 res.), 27.4, 28.8, 28.9, 29.1, 29.2, 29.3, 30.5, 31.1, 31.2, 32.3, 34.4, 61.6, 61.8, 61.9, 67.1, 79.2, 108.6, 125.6, 127.1, 128.5, 140.3, 142.1, 145.7, 149.8, 151.8, 156.1, 158.8 ppm; ESI-MS(+) m/z (%) [ion]: 900 (100) $[M-H]^+$; Anal. Calcd for $C_{65}H_{104}ClN_3O_7S$: C, 70.52; H, 9.47; N, 3.80. Found: C, 69.77; H, 9.12; N, 3.15 %.

General procedure for the synthesis of 12a and 12b: bromides **4a** or **4b** (0.3 mmol) and 4,4'-bipiridyne (1.0 mmol) were dissolved in dry acetonitrile (50 mL) and refluxed overnight. The solvent was then

removed under reduced pressure to afford a crude solid residue that was triturated with ethyl acetate and hexane (4 × 25 mL).

1-(3-{[(*tert*-butoxy)carbonyl] [6-(3,5-di-*tert*-butylphenoxy) hexyl]amino}hexyl–[4,4'-bipyridin]-1-ium bromide (12a): after suction filtration **12a** was obtained as a sticky yellow solid (52%). ^{1}H NMR (300 MHz, CD_3OD, δ): 1.30 (s, 18H), 1.30–1.6 (m, 21H), 1.78 (t, *J* =7.5 Hz, 2H), 2.19 (t, *J* =6.8 Hz, 2H), 3.22 (t, *J* = 7.3 Hz, 4H), 3.97 (t, *J* = 7.5 Hz, 2H), 4.75 (t, *J* = 6.8 Hz, 4H), 6.73 (s, 2H), 7.01 (s, 1H), 8.04 (d, *J* = 8 Hz, 2H), 8.56 (d, *J* = 8 Hz, 2H), 8.84 (d, *J* = 8 Hz, 2H), 9.19 (d, *J* = 8 Hz, 2H); ^{13}C NMR (75 MHz, CD_3OD, δ): 25.6 (2 res.), 26.3, 27.5, 28.3, 29.1, 30.6, 31.0, 31.1, 34.4, 46.5, 61.9, 67.4, 79.3, 108.6, 114.3, 122.3, 125.8, 142.2, 145.2, 150.4, 151.8, 153.5, 156.0, 158.8 ppm; ESI-MS(+) m/z (%) [ion]: 645 (100), 646 (95), 647 (80) $[M]^+$.

1-(3-{[(*tert*-butoxy)carbonyl] [11-(3,5-di-*tert*-butylphenoxy) undecyl]amino}dodecyl–[4,4'-bipyridin]-1-ium bromide (12b): after suction filtration **12b** was obtained as a sticky yellow solid (60%). ^{1}H NMR (400 MHz, $CDCl_3$, δ): 1.2–1.4 (m, 52H), 1.77 (t, *J* = 8 Hz, 2H), 2.08 (t, *J* =7 Hz, 2H), 3.18 (t, *J* = 7.4 Hz, 4H), 3.97 (t, *J* = 8 Hz, 2H), 4.73 (t, *J* = 7 Hz, 2H), 6.73 (s, 2H), 7.02 (s, 1H), 8.03 (d, *J* = 8 Hz, 2H), 8.55 (d, *J* = 8 Hz, 2H), 8.85 (d, *J* = 8 Hz, 2H), 9.17 (d, *J* = 8 Hz, 2H); ^{13}C NMR (100 MHz, $CDCl_3$, δ) 25.8, 26.5 (2 res.), 27.5, 28.8, 29.1, 29.2 (2 res.), 29.3, 29.4, 30.6, 31.1, 34.4, 61.3, 67.5, 79.4, 108.6, 114.5, 122.4, 126.1, 142.2, 145.5, 150.5, 152.0, 153.7, 156.2, 159.1 ppm; ESI-MS(+) m/z (%) [ion]: 799 (100) 800 (80) 801 (40) $[M]^+$.

General procedure for the supramolecularly assisted synthesis of *down* rotaxanes: wheel **Cx** (0.04 mmol), salt **12a** or **12b** (0.06 mmol) and bromide **13** (0.08 mmol) were suspended in dry toluene (15 mL), and the mixture was stirred for two days at 110°C. After few hours, the mixture turned red and homogeneous. The solvent was then removed under reduced pressure and the residue was portioned between dichloromethane and water. The separated organic phase was evaporated under reduced pressure, and crude product was purified by column chromatography (dichloromethane/methanol 50:1). Isolated Boc-protected rotaxane was then dissolved in 5 mL of dry dichloromethane and 5 mL of trifluoroacetic acid were added dropwise. The red solution turned yellow. After stirring at room temperature for 2 hours, the solvent was evaporated under reduced pressure to give the deprotected rotaxane.

R-DownShort: the rotaxane was isolated as a red solid (0.06 g, 58%). mp > 300 °C dec.; ^{1}H NMR (400 MHz, C_6D_6, δ): 0.76 (br. s, 2H), 0.9–1.0 (m, 9H), 1.1–1.4 and 1.35 (m, s, 61H), 1.6 (m, 2H), 1.63 (s, 18H), 1.8 (br. s, 2H), 1.9 (br. s, 8H), 2.00 (s, 6H), 2.2 (br. s, 4H), 2.9 (br. s, 2H), 3.2 (br. s, 2H), 3.4–3.5 (m, 8H), 3.8 (br. s, 6H), 3.8 (br. s, 2H), 3.9 (br. s, 2H), 3.93 (s, 9H), 4.03 (t, *J* = 7.2 Hz, 2H), 4.50 (t, *J* = 15 Hz, 6H), 5.12 (s, 1H), 6.6–6.7 (m, 5H), 6.82 (d, *J* = 5.2 Hz, 2H), 7.0 (br. s, 11H), 7.2 (br. s, 10H), 7.4–7.5 (m, 8H), 7.58 (s, 6H), 7.80 (d, *J* = 5.2 Hz, 2H), 7.9 (br. s, 6H), 8.03 (d, *J* = 5.2 Hz, 2H), 8.14 (d, *J* = 8 Hz, 4H), 9.2–9.6 (m, 7H); ^{13}C NMR (100 MHz, C_6D_6, δ): 14.1, 20.8, 22.8, 24.9, 25.5, 25.6, 25.9, 26.4, 26.7, 28.3, 29.3, 29.6, 29.8, 30.7, 31.3, 31.5, 32.0, 34.6, 34.8, 38.2, 46.8, 57.4, 60.5, 61.1, 64.7, 67.1, 73.3, 109.0, 114.8, 116.8, 118.1, 121.3, 124.8, 125.7, 126.4, 127.2, 128.6, 128.7 (2 res.), 128.8129.3, 132.0, 133.6, 137.4, 139.2, 139.7, 141.1, 142.9, 143.2, 144.3, 146.3, 148.3, 148.4, 152.1, 152.8, 153.3, 159.2, 172.0 ppm; HRMS (*m/z*): $[M]^{2+}$ calcd for $C_{158}H_{209}N_9O_{12}$, 1212.3005; found, 1212.3013

R-DownLong: product was isolated as a red solid (0.08 g, 69%). mp > 300 °C dec.; ^{1}H NMR (400 MHz, C_6D_6, δ): 0.7 (br. s, 2H), 0.9 (br .s, 2H), 0.99 (t, *J* = 6 Hz, 9H), 1.1–1.5 and 1.33 (m, s, 69H), 1.5–1.7 and 1.69 (m, s, 44H), 1.8 (br. s, 4H), 1.9 (br. s, 4H), 1.98 (s, 6H), 2.2 (br. s, 2H), 2.6 (br. s, 4H), 3.37 (d, *J* = 14.8 Hz, 6H), 3.6 (br. s, 2H), 3.7 (br. s, 6H), 3.8 (br. s, 2H), 3.9–4.0 (m, 11H), 4.04 (t, *J* = 6.8 Hz, 2H), 4.47 (d, *J* = 14.8 Hz, 6H), 5.13 (s, 1H), 6.55 (d, *J* = 5.2 Hz, 2H), 6.68 (t, *J* = 7.2 Hz, 3H), 6.85 (d, *J* =5.2 Hz, 2H), 6.93 (d, *J* = 8.4 Hz, 4H), 7.0–7.1 (m, 8H), 7.12 (s, 1H), 7.1–7.2 and 7.19 (m, s, 8H), 7.44 (d, *J* = 7.2 Hz, 6H), 7.58 (s, 6H), 7.72 (d, *J* = 5.2 Hz, 2H), 7.8 (br. s, 6H), 7.9 (br. s, 4H), 8.14 (d, *J* = 8.4 Hz, 4H), 9.3-9.6 (m, 7H); ^{13}C NMR (100 MHz, C_6D_6, δ): 14.1, 20.8, 22.8, 24.9, 25.5, 25.8, 26.4, 26.7 (2 res.), 26.9, 28.0, 28.3, 28.6, 29.1, 29.2, 29.5, 29.6, 29.7 (3 res.), 29.8 (2 res.), 29.9, 30.0, 30.4, 30.6, 30.8, 31.2, 31.3, 31.5, 31.7, 32.0, 34.6, 34.8, 47.2 (2 res.), 57.4, 60.5, 60.8, 61.1, 64.6, 67.4, 73.0,109.1, 114.6, 116.7, 118.0, 121.3, 124.7, 125.6, 125.4, 127.2, 127.6, 128.6, 128.7 (2 res.), 128.9, 129.3, 132.0, 133.7, 137.3, 139.2, 139.6, 141.0, 142.9, 143.1, 144.1, 147.9, 148.3, 152.0, 152.8, 153.2, 159.4, 172.0 ppm; HRMS (*m/z*): $[M]^{2+}$ calcd for $C_{169}H_{231}N_9O_{12}$, 1289.3866; found, 1289.3857.

General procedure for the synthesis of dumbbells DB-Short and DB-Long: 14 (1 eq.) and the appropriate alkylating agent (**4a** for **DB-Short** or **4b** for **DB-Long**, 2 eq.) were dissolved in 20 mL of dry acetonitrile and placed in a glass autoclave. After sealing the autoclave under inert atmosphere, the resulting reaction mixture was refluxed under stirring for 7 days. After this period, the reaction mixture was cooled to room temperature and the solvent was evaporated to dryness under reduced pressure. The crude residue was taken up with ethyl acetate (10 mL) and placed in a refrigerator. The solid that precipitated upon standing in the refrigerator was collected by Buchner filtration and then dissolved in dichloromethane (50 mL). The resulting solution was treated with 5 mL of trifluoroacetic acid and stirred at room temperature for 3 hours. After this period, the solvent was evaporated to dryness under reduced pressure to afford the dumbbells **DB-Short** and **DB-Long**.

DB-Short: (60%). ^{1}H NMR (400 MHz, CD_3OD, δ): 1.31 (s, 18H), 1.4–1.6 (m, 14H), 1.6 (br. s, 2H), 1.7 (br. s, 4H), 2.0 (br. s, 2H), 2.1 (br. s, 2H), 2.33 (s, 3H), 3.0 (br. s, 4H), 3.97 (t, *J* = 6 Hz, 2H), 4.16 (t, *J* = 6 Hz, 2H), 4.67 (t, *J* = 7.6 Hz, 2H), 4.77 (t, *J* = 7.6 Hz, 2H), 5.08 (s, 1H), 6.75 (s, 2H), 7.03 (s, 1H), 7.2–7.3 (m, 12H), 7.69 (d,*J* = 8 Hz, 2H), 8.64 (d, *J* = 6 Hz, 4H), 9.22 (d, *J* = 6 Hz, 2H), 9.28 (d, *J* = 6 Hz, 2H); ^{13}C NMR (100 MHz, CD_3OD, δ): 20.0, 24.8, 25.1, 25.2, 25.4 (2 res.), 25.8, 25.9, 27.9, 28.9, 30.5, 30.7, 30.9, 34.4, 56.9, 61.6, 61.7, 64.5, 67.2, 108.6, 114.4, 125.5, 126.9, 128.2, 128.3, 128.6, 138.9, 140.4, 142.3, 145.6, 145.7, 149.8, 149.9, 151.9, 158.8, 172.9 ppm; ESI-MS(+) m/z (%) [ion]: 839 (100) $[M-H]^+$.

DB-Long: (55%). ^{1}H NMR (400 MHz, CD_3OD, δ): 1.31 (s, 18H), 1.4–1.5 (m, 36H), 1.7 (br. s, 4H), 1.8 (br. s, 2H), 2.0 (br. s, 2H), 2.1 (br. s, 2H), 2.36 (s, 3H), 2.97 (t, *J* = 8 Hz, 4H), 3.97 (t, *J* =6.4 Hz, 2H), 4.17 (t, *J* = 6.4 Hz, 2H), 4.68 (t, *J* = 7.2 Hz, 2H), 4.74 (t, *J* = 7.2 Hz, 2H), 5.08 (s, 1H), 6.74 (s, 2H), 7.02 (s, 1H), 7.2–7.4 (m, 12H), 7.69 (d, *J* = 8 Hz, 2H), 8.65 (d, *J* = 6 Hz, 4H), 9.22 (d, *J* = 6 Hz, 2H), 9.26 (d, *J* = 6 Hz, 2H); ^{13}C NMR (100 MHz, CD_3OD, δ): 20.0, 24.8, 25.1, 25.8, 25.9, 26.2, 27.8, 28.8 (3 res.), 29.0, 29.1, 29.2 (2 res.), 30.5, 30.9, 31.2, 34.4, 56.9, 61.7, 61.9, 64.5, 67.5, 108.6, 114.3, 125.5, 126.9, 128.2, 128.3, 128.5, 138.9, 140.4, 145.7, 149.9 (2 res.), 151.8, 158.8, 172.9 ppm; ESI-MS(+) m/z (%) [ion]: 993 (100) $[M-H]^+$.

Electrochemical measurements and simulation. Cyclic voltammetric (CV) experiments were carried out at room temperature in argon-purged acetonitrile or acetone with an Autolab 30 multipurpose instrument interfaced to a PC using a glassy carbon as the working electrode, a Pt wire as the counter electrode, and an Ag wire as a quasi-reference electrode. The oxidation wave of ferrocene [$E_{1/2}(Fc^+/Fc)$ = +0.395 vs SCE], added as a standard, was used to calibrate the potential scale and assess electrochemical reversibility. The concentration of the compounds examined was in the range 2×10^{-4} M – 4×10^{-4} M, and tetraetylammonium hexafluorophosphate ($TEAPF_6$) 0.04 M was used as

the supporting electrolyte. Scan rates varying typically from 50 to 1000 mV s^{-1} were utilized. Differential pulse voltammograms (DPV) were performed with a scan rate of 20 mV s^{-1}, a pulse height of 75 mV, and a duration of 40 ms. For reversible processes the same halfwave potential values were obtained from the DPV peaks and from an average of the cathodic and anodic CV peaks. The potential values for not fully reversible processes were estimated from the DPV peaks. The experimental error on the potential values was estimated to be ±10 and ±20 mV, respectively. Digital fitting of the experimental CV for the **R-UpShort** system was obtained on the basis of the square scheme mechanism illustrated in Figure 5 by using the software package DigiSim 3.05.[48] The redox potentials were fixed in the simulation and the shuttling equilibrium constant in the monoreduced form was fixed to 10; shuttling rate constants were optimized in the simulation. A value of 1 cm s^{-1}, representative of a reversible process under our conditions was employed for the electron transfer rates.[49] The charge-transfer coefficients were taken as 0.5 in all cases.

EPR measurements. EPR spectra were recorded at room temperature using an ELEXYS E500 spectrometer equipped with a NMR gaussmeter for the calibration of the magnetic field and a frequency counter for the determination of g-factors that were corrected against that of the perylene radical cation in concentrated sulfuric acid (g = 2.002583). The electrochemical cell was homemade and consisted of an EPR flat cell (Wilmad WG-810) equipped with a 25 × 5 × 0.2 mm platinum gauze (cathode), and a platinum wire (anode).[50,51] The current was supplied and controlled by an AMEL 2051 general-purpose potentiostat. In a typical experiment, the cell was filled with an acetonitrile solution of the appropriate substrate (ca. 1 mM) containing tetrabutylammonium perchlorate (ca. 0.1 M) as supporting electrolyte. After thoroughly purging the solution with N_2, spectra were recorded at different potential settings in the range 0 to –0.8 V. An iterative least-squares fitting procedure based on the systematic application of the Monte Carlo method was performed to obtain the experimental spectral parameters of the radical species.[52]

Acknowledgements

The authors thank *Centro Interdipartimentale di Misure* of the University of Parma for NMR and MS measurements. This work was supported by the Italian MIUR (PRIN 2010CX2TLM) and the Universities of Parma and Bologna (FARB SLaMM project).

Keywords: calixarenes • molecular machines • switches • rotaxanes • EPR measurements

References

[1] S. Kassem, T. van Leeuwen, A. S. Lubbe, M. R. Wilson, B. L. Feringa, D. A. Leigh, *Chem. Soc. Rev.* **2017**, *46*, 2592–2621.
[2] S. Silvi, M. Venturi, A. Credi, *J. Mater. Chem.* **2009**, *19*, 2279.
[3] W. R. Browne, B. L. Feringa, *Nat. Nanotechnol.* **2006**, *1*, 25–35.
[4] S. Erbas-Cakmak, D. A. Leigh, C. T. McTernan, A. L. Nussbaumer, *Chem. Rev.* **2015**, *115*, 10081–10206.
[5] B. L. Feringa, W. R. Browne, *Molecular Switches*, Wiley-VCH, **2011**.
[6] P. L. Anelli, N. Spencer, J. F. Stoddart, *J. Am. Chem. Soc.* **1991**, *113*, 5131–5133.
[7] A. P. de Silva, I. M. Dixon, H. Q. N. Gunaratne, T. Gunnlaugsson, P. R. S. Maxwell, T. E. Rice, *J. Am. Chem. Soc.* **1999**, *121*, 1393–1394.
[8] I. Willner, B. Basnar, B. Willner, *Adv. Funct. Mater.* **2007**, *17*, 702–717.
[9] H. Hess, J. Clemmens, D. Qin, J. Howard, V. Vogel, *Nano Lett.* **2001**, *1*, 235–239.
[10] J. Berná, D. A. Leigh, M. Lubomska, S. M. Mendoza, E. M. Pérez, P. Rudolf, G. Teobaldi, F. Zerbetto, *Nat. Mater.* **2005**, *4*, 704–710.
[11] C. J. Bruns, J. F. Stoddart *The Nature of the Mechanical Bond: From Molecules to Machines*, Wiley, **2016**.
[12] T. Ogoshi, D. Yamafuji, T. Aoki, T. Yamagishi, *Chem. Commun.* **2012**, *48*, 6842.
[13] A. Caballero, L. Swan, F. Zapata, P. D. Beer, *Angew. Chem. Int. Ed.* **2014**, *53*, 11854–11858.
[14] E. M. Lewis , M. Galli, S. M. Goldup, *Chem. Commun.*, **2017**, *53*, 298.
[15] A. Altieri, F. G. Gatti, E. R. Kay, D. A. Leigh, D. Martel, F. Paolucci, A. M. Z. Slawin, J. K. Y. Wong, *J. Am. Chem. Soc.* **2003**, *125*, 8644–8654.
[16] A. M. Brouwer, C. Frochot, F. G. Gatti, D. A. Leigh, L. Mottier, F. Paolucci, S. Roffia, G. W. H. Wurpel, *Science ~~(80-.)~~*. **2001**, *291*, 2124-2128.
[17] a) V. Balzani, A. Credi, M. Venturi, *Chem. Soc. Rev.* **2009**, *38*, 1542–50; b) V. Balzani, A. Credi, M. Clemente-León, B. Ferrer, M. Venturi, A. H. Flood, J. F. Stoddart, *Proc. Natl. Acad. Sci. U.S.A.*, **2006**, *103*, 1178-1186.
[18] a) P. R. Ashton, R. Ballardini, V. Balzani, I. Baxter, A. Credi, M. C. T. Fyfe, M. T. Gandolfi, M. Gómez-López, M.-V. Martínez-Díaz, A. Piersanti, et al., *J. Am. Chem. Soc.* **1998**, *120*, 11932–11942; b) S Erbas-Cakmak, S D P Fielden, U Karaca, D A Leigh, C T McTernan, D J Tetlow and M R Wilson, *Science*, **2017**, *358*, 340-343.
[19] G. Ragazzon, M. Baroncini, S. Silvi, M. Venturi, A. Credi, *Nat. Nanotechnol.* **2014**, *10*, 70–75.
[20] J. V Hernández, E. R. Kay, D. A. Leigh, *Science* **2004**, *306*, 1532–7.
[21] M. von Delius, E. M. Geertsema, D. A. Leigh, *Nat. Chem.* **2010**, *2*, 96–101.
[22] D. A. Leigh, J. K. Y. Wong, F. Dehez, F. Zerbetto, *Nature* **2003**, *424*, 174–179.
[23] C. Casati, P. Franchi, R. Pievo, E. Mezzina, M. Lucarini, *J. Am. Chem. Soc.* **2012**, *134*, 19108–19117.
[24] P. Waelès, K. Fournel-Marotte, F. Coutrot, *Chem. - Eur. J.* **2017**, *23*, 11529–11539.
[25] R. A. Bissell, E. Córdova, A. E. Kaifer, J. F. Stoddart, *Nature* **1994**, *369*, 133–137.
[26] T. Oshikiri, Y. Takashima, H. Yamaguchi, A. Harada, *J. Am. Chem. Soc.* **2005**, *127*, 12186–12187.
[27] W. P. Joon, J. S. Hyun, *Org. Lett.* **2004**, *6*, 4869–4872.
[28] a) C. Talotta, C. Gaeta, P. Neri, *Org. Lett.* **2012**, *14*, 3104–3107; b) T. Pierro, C. Gaeta, C. Talotta, A. Casapullo, P. Neri, :Org. Lett. **2011**, *13*, 2650; c) R. Ciao, C. Talotta, C. Gaeta, L. Margarucci, A. Casapullo, P. Neri, *Org. Lett.* **2013**, 15, 5694–5697.
[29] H.-X. Wang, Z. Meng, J.-F. Xiang, Y.-X. Xia, Y. Sun, S.-Z. Hu, H. Chen, J. Yao, C.-F. Chen, *Chem. Sci.* **2016**, *7*, 469–474.
[30] T. Oshikiri, H. Yamaguchi, Y. Takashima, A. Harada, *Chem. Commun.* **2009**, *0*, 5515.
[31] A. Arduini, R. Bussolati, A. Credi, S. Monaco, A. Secchi, S. Silvi, M. Venturi, *Chem. - A Eur. J.* **2012**, *18*, 16203–16213.
[32] A. Arduini, R. Bussolati, A. Credi, A. Pochini, A. Secchi, S. Silvi, M. Venturi, *Tetrahedron* **2008**, *64*, 8279–8286.
[33] V. Zanichelli, G. Ragazzon, A. Arduini, A. Credi, P. Franchi, G. Orlandini, M. Venturi, M. Lucarini, A. Secchi, S. Silvi, *Eur. J. Org. Chem.* **2016**, *2016*, 1033–1042.
[34] A. Credi, S. Dumas, S. Silvi, M. Venturi, A. Arduini, A. Pochini, A. Secchi, *J. Org. Chem.* **2004**, *69*, 5881–5887.
[35] A. Arduini, F. Calzavacca, A. Pochini, A. Secchi, *Chem. - A Eur. J.* **2003**, *9*, 793–799. [36] A. Arduini, F. Ciesa, M. Fragassi, A. Pochini, A. Secchi, *Angew. Chem. Int. Ed.* **2005**, *44*, 278–281.
[37] G. Orlandini, G. Ragazzon, V. Zanichelli, A. Secchi, S. Silvi, M. Venturi, A. Arduini, A. Credi, *Chem. Commun.* **2017**, *53*, 6172–6174.

[38] V. Zanichelli, G. Ragazzon, G. Orlandini, M. Venturi, A. Credi, S. Silvi, A. Arduini, A. Secchi, *Org. Biomol. Chem.* **2017**, *15*, 6753–6763.
[39] A. Arduini, R. Ferdani, A. Pochini, A. Secchi, F. Ugozzoli, *Angew. Chem. Int. Ed.* **2000**, *39*, 3453–3456.
[40] A. Arduini, R. Bussolati, A. Credi, A. Secchi, S. Silvi, M. Semeraro, M. Venturi, *J. Am. Chem. Soc.* **2013**, *135*, 9924–9930.
[41] M. Semeraro, A. Arduini, M. Baroncini, R. Battelli, A. Credi, M. Venturi, A. Pochini, A. Secchi, S. Silvi, *Chem. - A Eur. J.* **2010**, *16*, 3467–3475.
[42] R. Ballardini, A. Credi, M. T. Gandolfi, C. Giansante, G. Marconi, S. Silvi, M. Venturi, *Inorganica Chim. Acta* **2007**, *360*, 1072–1082.
[43] A. Arduini, R. Bussolati, A. Credi, G. Faimani, S. Garaudée, A. Pochini, A. Secchi, M. Semeraro, S. Silvi, M. Venturi, *Chem. - A Eur. J.* **2009**, *15*, 3230–3242.
[44] T. Belser, M. Stöhr, A. Pfaltz, *J. Am. Chem. Soc.* **2005**, *127*, 8720–8731.
[45] M. Yoritate, T. Meguro, N. Matsuo, K. Shirokane, T. Sato, N. Chida, *Chem. - A Eur. J.* **2014**, *20*, 8210–8216.
[46] A. Boccia, V. Lanzilotto, V. Di Castro, R. Zanoni, L. Pescatori, A. Arduini, A. Secchi, *Phys. Chem. Chem. Phys.* **2011**, *13*, 4452–4462.
[47] J. J. González, R. Ferdani, E. Albertini, J. M. Blasco, A. Arduini, A. Pochini, P. Prados, J. de Mendoza, *Chem. - A Eur. J.* **2000**, *6*, 73–80.
[48] *DigiSim 3.05*; BioAnalytical Systems: West Lafayette, IN (USA); see: www.bioanalytical.com
[49] A. J. Bard, L. R. Faulkner, *Electrochemical Methods. Fundamentals and Applications*; Wiley: New York, 1980. Chapter 6.
[50] A. Alberti, M. Benaglia, P. Hapiot, A. Hudson, G. Le Coustumer, D. Macciantelli, S. Masson, *J. Chem. Soc. Perkin Trans. 2* **2000**, 1908–1913.
[51] C.Boga, M. Calvaresi, P. Franchi, M. Lucarini, S. Fazzini, D. Spinelli, D. Tonelli, *Org. Biomol. Chem.* **2012**, *10*, 7986-7995.
[52] P. Franchi, E. Mezzina, M. Lucarini, *J. Am. Chem. Soc.* **2014**, *136*, 1250–1252.

10.1002/chem.201800496

WILEY-VCH

FULL PAPER

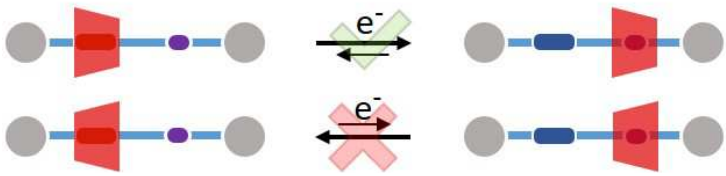

One-way rotaxanes: a series of isomeric and redox-switchable calix[6]arene-based rotaxanes have been synthesized with a reagent-less strategy. It was demonstrated that the orientation of the calix[6]arene wheel can give rise to a thermodynamic preference for shuttling among orientational isomers.

Valeria Zanichelli, Margherita Bazzoni, Arturo Arduini, Paola Franchi, Marco Lucarini, Giulio Ragazzon, Andrea Secchi,* and Serena Silvi**

Page No. – Page No.

Redox-Switchable Calix[6]Arene-based Isomeric Rotaxanes